Substrate-mediated and temperature-modulated long-range interactions between bromine adatom stripes on Cu(111)

Zhao, Yan Ling; Zhao, Rundong; Qi, Fei; Zhang, Rui Qin; VAN HOVE, M. A.

Document Version:
Peer reviewed version

Link to publication

Substrate-mediated and temperature-modulated long-range interactions between bromine adatom stripes on Cu(111)

Yan-Ling Zhao,[†,§,∥] Rundong Zhao,[†] Fei Qi,[†] Rui-Qin Zhang,[*,§,∥] and Michel A. Van Hove[*,†]

[†]Institute of Computational and Theoretical Studies & Department of Physics, Hong Kong Baptist University, Hong Kong SAR, China

[§]Department of Physics, City University of Hong Kong, Hong Kong SAR, China

[∥]Shenzhen Research Institute, City University of Hong Kong, Shenzhen, China

ABSTRACT: Understanding long-range adsorbate-adsorbate interactions on surfaces, such as halogens on metal surfaces, is important in the fields of electrochemistry, catalysis, and thin film growth. In this work, we computationally studied bromine (Br) stripe formations on Cu(111). These stripes are found to be surface-mediated and temperature-modulated; they are facilitated by Br-Cu bonding guided by self-patterning of Cu(111) surface frontier orbitals and by strain release induced stripe migration in a thermal bath. The calculated surface wave-functions in frontier occupied states show stripe-like electron distributions and thus the favorable sites of Br adsorptions on Cu(111) are also stripe-like. The temperature effect is notable in that the thermal energy of 50 K easily dominates Br stripe gathering in ($\sqrt{3} \times \sqrt{3}$)R30° structures. Corresponding electron stripes on the surface could be generated, widened, shrunk or removed depending on spacing changes of Br stripes, thus reflecting diverse and changeable formation features for dynamic patterns of adsorbates on Cu(111).

*Corresponding Authors:

Prof. Michel A. Van Hove, Hong Kong Baptist University, Institute of Computational and Theoretical Studies & Department of Physics, 224 Waterloo Road, Kowloon Tong, Hong Kong, China. E-mail: vanhove@hkbu.edu.hk. Tel: (852) 3411-2766. Fax: (852) 3411-2761.

Prof. Rui-Qin Zhang, City University of Hong Kong, Department of Physics, 83 Tat Chee Avenue, Kowloon Tong, Hong Kong, China. E-mail: aprqz@cityu.edu.hk. Tel: (852) 3442-7849. Fax: (852) 3442-0538.

1. Introduction

Understanding adsorbate-adsorbate interactions on surfaces is of great importance in the fields of electrochemistry, surface catalysis, and thin film growth for industrial processes, and thus has become a basic research focus. In studies of many adsorbates [1-6], it was observed that surface structures including island-, stripe- and bubble-like patterns are ubiquitous on surfaces. The common question arose why the islands do not grow but instead turn to isolated stripes or bubbles with increasing monolayer coverage, thus calling for a convincing explanation.

For several decades, inhomogeneous adsorption of halogen atoms on metal surfaces has been experimentally studied to accurately determine the adsorbate structure by means of low energy electron diffraction (LEED), scanning tunneling microscopy (STM), X-ray photoelectron spectra (XPS) and other techniques [7-13]. For instance, Jones *et al.* [8] studied the dissociative chemisorption of molecular bromine on Cu(111) at 300 K and interestingly found that a ($\sqrt{3} \times \sqrt{3}$)R30° structure was formed initially at a bromine (Br) monolayer coverage of 1 ML (1 ML is defined in this work as Br atoms covering the surface at a ratio of one Br for three substrate atoms, which corresponds to the ($\sqrt{3} \times \sqrt{3}$)R30° ordered structure, relative to the (1×1) clean-Cu(111) lattice). This particular arrangement results from competing interactions between Br adsorbates through van der Waals (VdW) attraction and dipole-dipole repulsion, yielding the ($\sqrt{3} \times \sqrt{3}$)R30° lattice at cryogenic temperatures. However, these interactions are basically effective over a short range of less than 0.5 nm [10], which should therefore not dominate longer-range adsorbate formations observed in experiments.

Some studies [10, 14-17] have already suggested that long-range interactions strongly influence adsorbate ordering on metals, using STM techniques and theoretical derivations. For larger halogen separations at nanometer scales, the indirect interactions might dominate due to partial filling of the surface-state band, as previously predicted by Lau and Kohn [14] and later confirmed by Nanayakkara *et al.* [10] who experimentally studied the long-range interaction between Br islands adsorbed on Cu(111). The latter found that the nearest neighbor spacing between islands tends to be half-multiples of the Fermi wavelength of Cu(111) (λ_F=3.0 nm), with the local minima of the oscillating interaction

potential energy occurring at approximately 1.2, 2.6, 4.1, and 5.6 nm. The surface-state electronic wave function behaves as a two-dimensional nearly free electron gas [15-17] and the long-range interactions are relatively insensitive to the adatoms, depending more on the substrate surface-state electrons [15].

Computational techniques, such as density functional theory (DFT), are becoming more and more powerful to interpret experimental observations. Thus, there have been many related studies of adsorbate bonding with surfaces, electronic structure and phase diagrams, intermediate dynamic and kinetic instability, and energetics on substrates [11,18-26]. As a result, Pašti *et al.* [18] have confirmed the most favorable halogen binding site to be the 3-fold hollow site (fcc or hcp) of the surfaces for halogen (Cl, Br, I) adsorption on crystallographic (111) planes of Pd, Pt, Cu, and Au, with binding energies in the order fcc hollow site ≈ hcp hollow site > bridge site > top site, from most favorable to least favorable. The adsorption energies decrease as the size of the halogen atoms increases and are correlated to the position of the *d*-band of the surface atoms. As revealed by first-principles calculations [19], the adsorption energy of Cl atoms on the substrate Mg (0001) decreases and the repulsion between Cl atoms becomes stronger with increasing adsorbate coverage. In a cluster-model study [20], it was found that the interaction and bonding arise almost entirely from the Coulomb attraction between the anionic halogen and the Cu metal, and from the electron polarization associated within the local interacting unit. In the DFT study of Doll *et al.* [24], the Cl-Ag bonding nature for the adsorption of Cl on Ag(111) was also found to be more likely ionic than covalent. As the metal surface electrons are easily polarized, the long-range interactions between adsorbates are commonly supposed to be substrate-mediated. These results provide guidance and a preliminary basis for our work, although few studies have focused on long-range interactions between adsorbates due to the challenge of time-consuming computations.

Moreover, the surface corrugation is probably uneven in the real situation and halogen adsorbates may diffuse among fcc, hcp and bridge sites so as to locally rearrange on the substrate. This is the so-called indirect elastic interaction through substrate distortion, as revealed by Zheltov *et al.* [26] who found a structural paradox (chainlike structures with abnormally short distances of 0.38 nm between Cl atoms) at submonolayer coverage of Cl

on Au(111). There may be multiple formation factors for determining the morphologies of adsorbates on surfaces. More evidence is needed to address this issue.

2. Computational details

To help clarify the mechanism of adsorbate interactions over long-range distances, we utilized first-principles DFT calculations and molecular dynamics (MD) simulations to study Br stripe dispersions on Cu(111) at low coverages as an example. We carried out calculations using a large model at nanometer scale. The calculations were done using the SIESTA code [27] which adopts the DRSLL exchange-correlation functional with the capability to include VdW interactions [28,29], and double zeta plus polarization orbitals as the basis set. The detailed parameters used in the calculations include a maximal force threshold of 0.02 eV/Å, a projected atomic orbital energy shift of 10 meV, and a maximal displacement tolerance of 10^{-4} Å. Note that SIESTA has been successfully applied in many DFT studies of adsorbates-surface interactions [30-32]. The pseudopotential (PS) of Br was generated by ourselves. By the transferability test, the radius cut off for s, p, d and f orbitals of Br were respectively set as 1.9, 2.0, 2.2 and 2.9 Bohr and the PS-AE (all electrons) eigenvalue differences are less than 1 mRy, guaranteeing to achieve the standard accuracy.

3. Results and discussion

To determine the possible deposition sites of Br on Cu(111), we firstly study the chemical reactivity of the Cu(111) using frontier orbital theory [33] by examining the energy levels and spatial distributions of frontier molecular orbitals (FMOs) for Br atoms without a Cu(111) surface, for a Br-free Cu(111) surface, and for Cu(111) covered with one dimensional one-atom-wide Br stripes. The Cu(111) model is built with a 2D unit cell of size $(20\sqrt{3}\times4\sqrt{3})R30°$ in order to exhibit longer-range interactions between stripes. The Cu(111) is composed of three layers of Cu atoms. Lattice parameters are a=8.854 nm, b=1.771 nm, c=5.0 nm, α=β=90°, γ=120°. To reduce the computational time, we only perform single-point total energy calculations based on large supercells enlarged from small locally-equilibrated geometries. The resulting energy levels of separated Br and Cu(111) as well as for combined Cu(111)-Br in Figure 1 indicate preferred interaction, due

to close energy levels, between the SOMO (singly occupied MO) of Br and the HOMO (highest occupied MO) or nearby occupied MOs of Cu(111) and Br-covered Cu(111). Many occupied FMOs below the Fermi level are clearly stripe-like, as illustrated in Figure 2. Clearly, on Br-free Cu(111), other identical orbitals exist in two other symmetry-equivalent directions or translated along the surface by any Cu-Cu lattice vector. This thus reflects that Br stripes can extend to larger widths on Cu(111) in the ($\sqrt{3}\times\sqrt{3}$)R30° ordered structure or be isolated in the vicinity of the Br stripe on Cu(111). The various stripe-shaped FMOs also indicate the non-negligible possibilities of multi-interval Br stripes on the surface. We thus suppose that Br stripe intermediates are substrate-mediated by stripe-like MO wave-functions, which donate surface electrons to the Br atoms by forming Cu(δ^+)-Br(δ^-) bonds. We also predict that one might be able to artificially control the Br stripes on the surface by tuning the orbitals of the surface Cu in the experiment such as by means of applied magnetic fields [2,3].
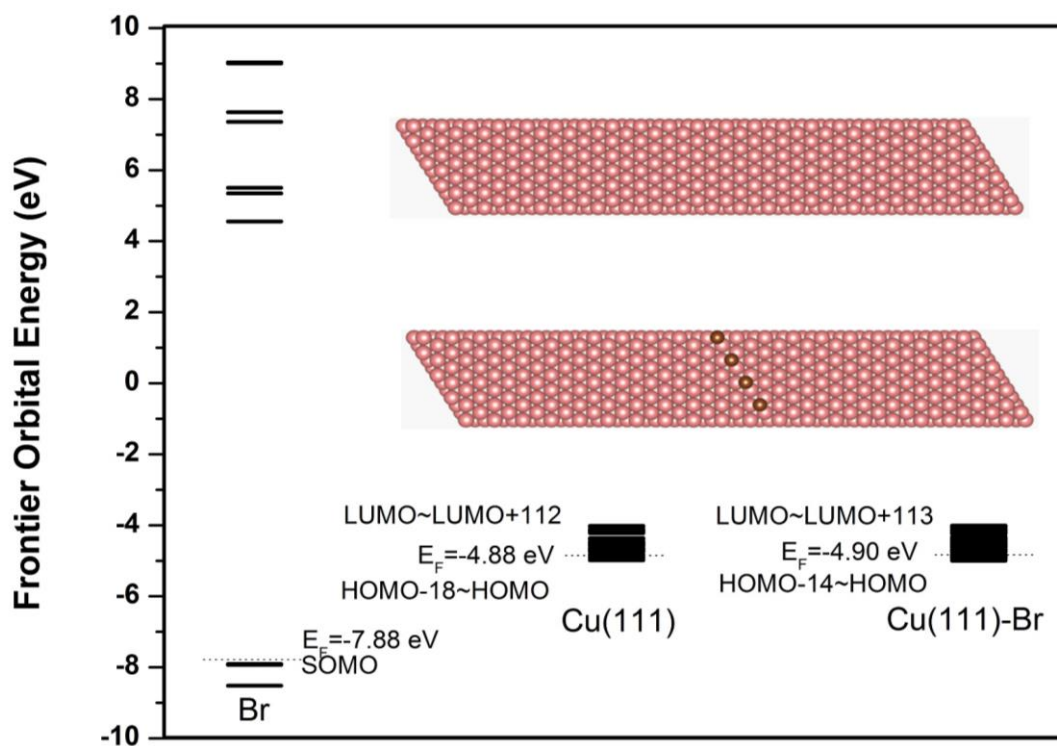

Figure 1. Energy levels of an isolated Br atom (left) and of frontier molecular orbitals in the range of -5 to -4 eV for Br-free Cu(111) (middle) and Cu(111) with one infinite Br stripe (right) from DFT calculations. A Cu(111) model with three Cu layers seen in top
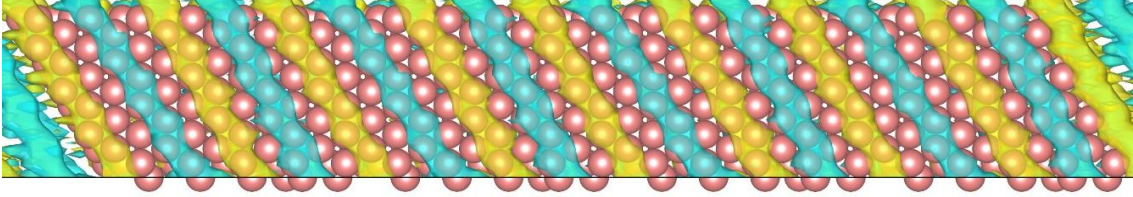
view is illustrated with a unit cell size of (20 √3×4 √3)R30° (top right) and with an additional Br stripe (middle right); Cu and Br are colored in red and brown, respectively.
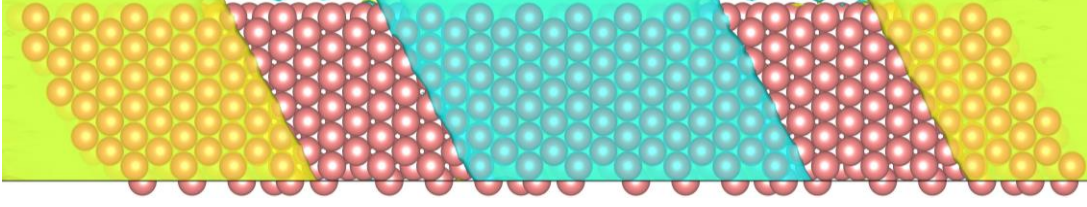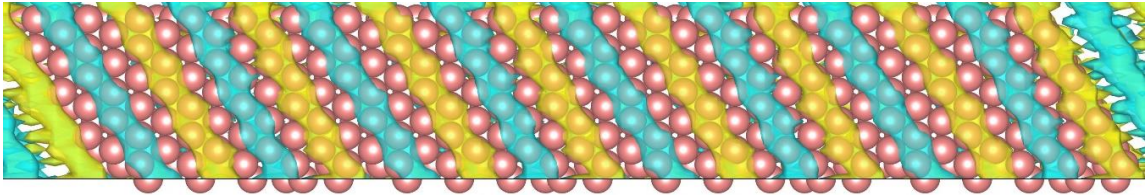

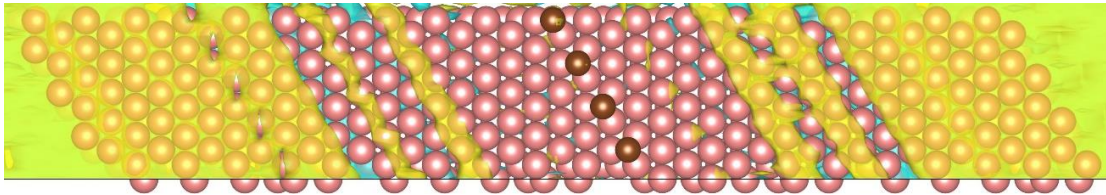(a) HOMO-7 of Cu(111) (-4.9195 eV)
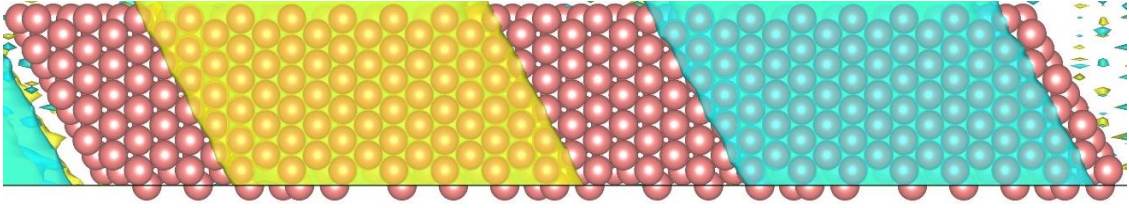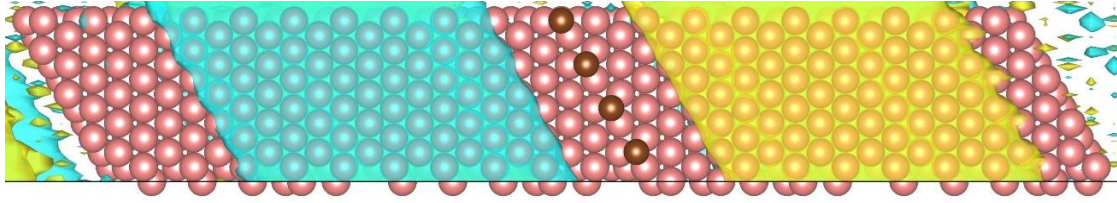

(b) HOMO-6 of Cu(111) (-4.9194 eV)

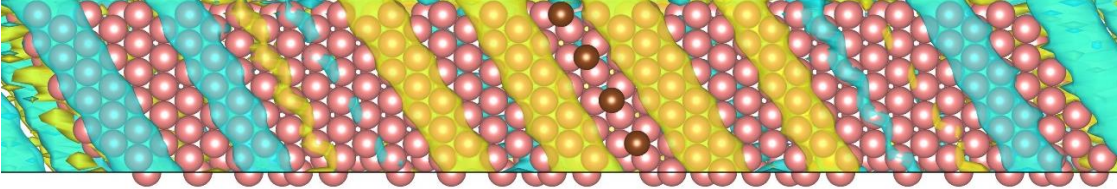(c) HOMO-2 of Cu(111) (-4.9053 eV)

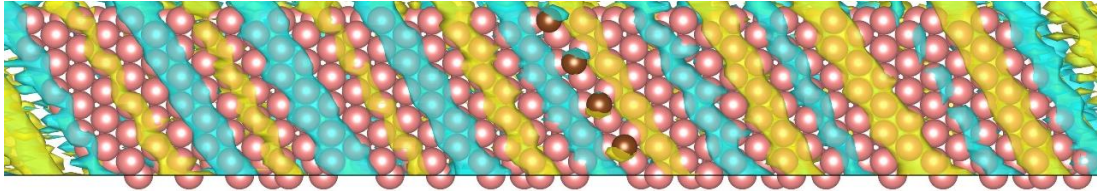(d) HOMO of Cu(111) (-4.9019 eV)

(e) HOMO-13 of Cu(111)-Br (-4.9944 eV)

(f) HOMO-8 of Cu(111)-Br (-4.9460 eV)

(g) HOMO-6 of Cu(111)-Br (-4.9305 eV)

(h) HOMO of Cu(111)-Br (-4.9008 eV)

Figure 2. *A selection of a few among many distinctly stripe-shaped frontier OMOs below the Fermi levels on a (20√3×4√3)R30° unit cell of three-layer Cu(111) (panels (a)-(d)) and on Cu(111) with one infinite Br stripe in the center (panels (e)-(h)), from DFT calculations with the energy cutoff 300 Ry. The MO energy eigenvalues are shown in parentheses. Each orbital is shown in top view and Cu and Br atoms are colored in red and brown, respectively. Yellow and blue striped regions represent the MO wave-function with opposite phases. The isovalue is set as 0.003 a.u. to give a clearer illustration.*

The FMOs depicted in Figure 2 reflect the substrate-mediated distributions for Br adatom stripes. To accurately study the interaction energies between Br stripes or between Br stripes and Cu(111), a smaller model with unit cell (10√3×√3)R30° Cu(111) was adopted with the lattice parameters a=4.427 nm, b=0.4427 nm, c=5.0 nm, and $\alpha=\beta$=90°, γ=120° (cf. Figure 3a). The Cu(111) is composed of four layers with the first layer fully relaxed and the deeper three layers fixed in the optimizations. In this model, all Br stripes are one-atom-wide linear strings of Br atoms (as in Figures 1 and 2); we kept one such Br stripe (as well as its periodic counterparts described in the caption of Figure 3) attached at

an fcc site (brown atom at left in Figure 3a), while putting a second identical Br stripe to other fcc sites (shown by arrows in Figure 3a) to sample various realistic Br-Br distances in the range 0.25–3.97 nm (note that beyond 2.21 nm the structures repeat by mirror symmetry due to the finite unit cell, but with slight numerical asymmetry). Numbers in Figure 3a show equilibrated distances from DFT optimizations in nm, measured from the drawn Br stripe at left; the intervals are not strictly equal due to the impact from local surface strains. Both Br stripes are also periodically repeated to the right and left with the lattice parameter a. Thus, when the second stripe is at position 2.21 nm, it lies midway between the first stripe and its periodic counterpart to the right (just outside the figure). (Unlike in Figure 1, here only a narrower slice of the surface with two single Br atoms is studied.)

To find the most favorable spacing between two Br stripes, the relative total energies were calculated and compared, as shown in Figure 3b. With the energy cutoff of 300 Ry, two favorable stripe distances are found, 1.11 nm and 1.77 nm, as well as their symmetry-equivalent distances, 3.32 nm and 2.65 nm. The distance 1.11 nm is slightly more favorable than 1.77 nm. This 1.11 nm value matches well the nearest inter-island distance of 1.2 nm mentioned previously for Br islands [10] and thus suggests a constant stripe separation despite varying Br coverage. However, the differences in total energy are minor, varying in the range from -40 to 20 meV (except for the Cu-bulk-like distance of 0.25 nm). This implies that the equilibrated geometries of Br stripes on Cu(111) at long-range distances may also be sensitive to other low-energy effects, such as thermal disturbance, surface electron polarization, substrate distortion or defects. Namely, such small energy differences reflect that the potential energy would not be the only factor influencing which long-range distances between Br stripes would dominate on the surface in real situations. For example, in a cryogenic STM, although the system is usually slowly cooled down in order not to be dramatically perturbed by kinetic energy, the temperature effect still exists and is non-negligible. (The high single-point total energy at 0.25 nm, ~4.6 eV above all the other total energies, reflects strong Br-Br repulsion at 0.25 nm, which is the bulk Cu-Cu lattice constant a in the surface plane, precluding the formation of a (1×1) overlayer, in agreement with the previous experiments [8,10]. Our following simulations were thus

carried out starting from the ~√3a distance of 0.45 Å, corresponding to the (√3×√3)R30°
superstructure.)
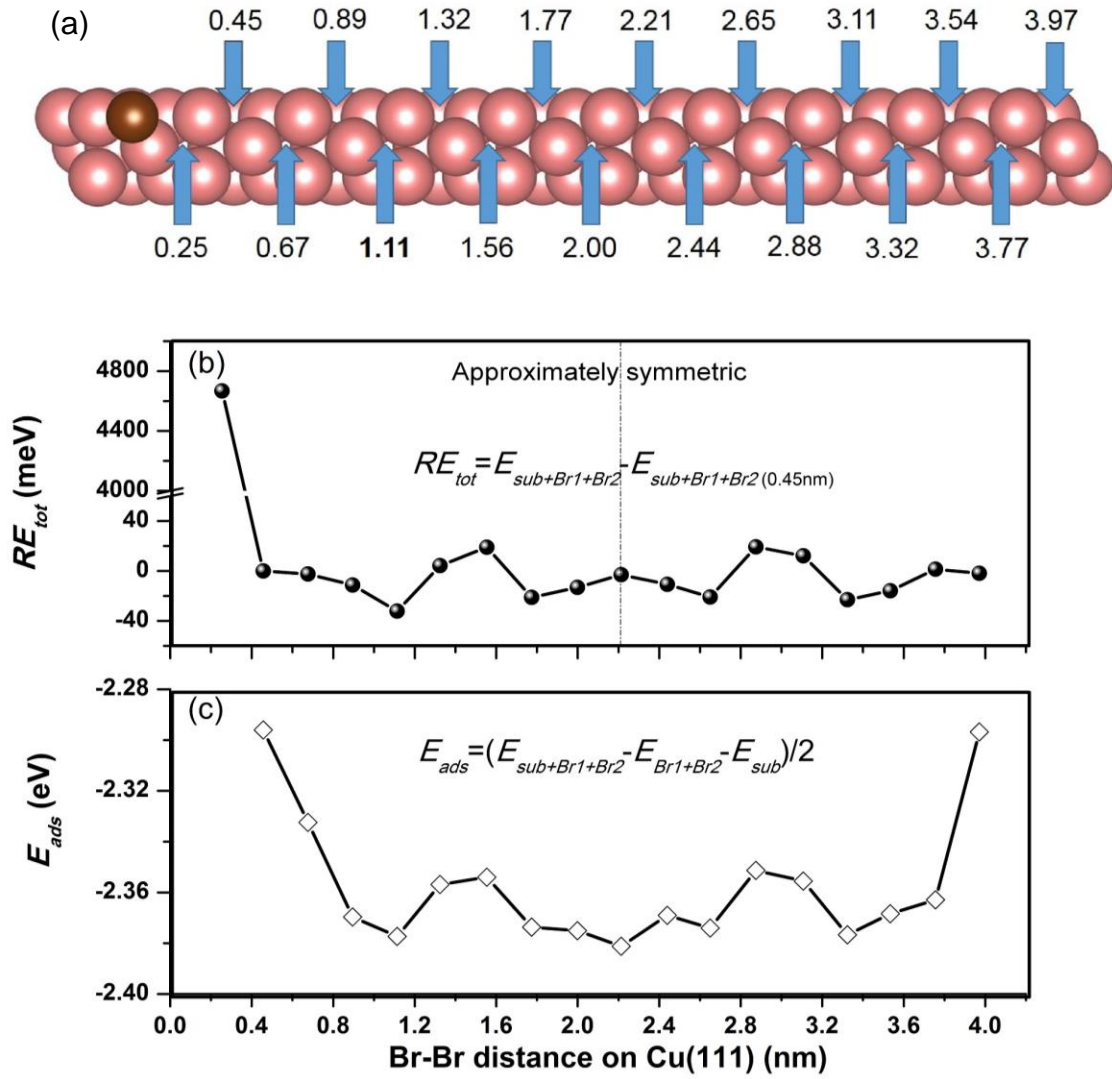
*Figure 3. (a) Top view of attachment positions for two Br stripes on a (10 √3× √3)R30° unit cell of Cu(111) with lattice parameters a=4.427 nm, b=0.4427 nm, c=5.0 nm, and α=β=90°, γ=120°. One Br stripe is built by periodically repeating the single brown Br atom diagonally up and down the figure with the lattice parameter b, as illustrated in Figure 1; the other Br stripe is similarly built from a second Br atom placed at various positions shown by arrows. As a function of Br-Br distance, (b) shows total energies relative to that at 0.45 nm, and (c) adsorption energies per Br stripe on Cu(111), as defined*

by the inset formula (cf. text) and averaged over the two stripes to reduce numerical uncertainties.

The Br binding strength to the surface may affect the spatial dispersion of the Br stripes. We firstly estimated the Br stripe adsorption energy per $(10\sqrt{3}\times\sqrt{3})R30°$ unit cell (E_{ads}) through $E_{ads} = (E_{sub+Br1+Br2} - E_{Br1+Br2} - E_{sub})/2$, where $E_{sub+Br1+Br2}$ is the energy of the fully optimized complete system, $E_{Br1+Br2}$ is the total energy of two frozen Br stripes, which have retained their mutual positions after removal of all Cu atoms, and E_{sub} is the total energy of the frozen substrate after removal of the Br stripes. The division by 2 yields the average adsorption energy for each Br stripe. As shown in Figure 3c, E_{ads} for each Br binding with three Cu at fcc sites varies from -2.38 to -2.30 eV. The adsorption energy becomes more favorable beyond a Br-Br distance of about 0.8 nm, after which distance it fluctuates slightly by about 10 meV. We find a local minimum of E_{ads} at 1.11 nm. The adsorption energy appears to flatten out beyond about 1.6 nm; this flattening is likely due to the growing influence of the next fixed stripe at 4.427 nm, suggesting a decaying interaction between more widely separated Br stripes beyond about 2 nm. This calculated behavior is consistent with the experimental pair correlation functions [10], which shows an exclusion zone below about 1 nm.

The above electronic structures and potential energy results merely verify the long-range spatial dispersion of Br stripes on the surface in a thermodynamic equilibrium state. Basically, surface structures were formed though a slowly annealing process from high to low temperature in experiments, implying the non-negligible temperature effect. We thus next study the temperature effect on the interactions between Br stripes on Cu(111) in cryogenic STM conditions. We accomplished a number of first-principles MD simulations [34-39] for ~3.5 ps using the canonical ensemble with the Nosé thermostat [40-41] in a regime with constant particle number, constant volume and constant temperature (NVT). The thermostat was set to $T = 50$ K with a time step of 1 fs for the integration of the equations of motion. We chose 50 K because it is not only a feasible temperature for STM, but also convenient for observing the behavior of Br stripes in the limited first-principles MD simulation time. The MD simulations start from eight equilibrated configurations at the distances of 0.45–2.0 nm. As shown in Figure 4, the seven trajectories (except for 0.45

nm, which corresponds to the close-packed (√3×√3)R30° structure) move immediately to the next shorter distance within ~1000 fs, but mostly remain unchanged for the next 2000 fs. This may be due to the large temperature fluctuation (cf. Figure S1) at the beginning of the MD simulations resulting in the velocities of Br atoms being large enough to overcome the barrier between two adjacent hollow sites. Importantly, the time evolution of the distances consistently reflects the ultimate aggregation trend of Br stripes into regions of (√3×√3)R30° surface structures as driven by such a small kinetic energy. For example, the trajectory starting at 0.67 nm merges into that at 0.45 nm; all the other Br stripe distances would be finally reduced to ~0.45 nm given a long enough simulation time, as evidenced by the 2.0 nm distance trajectory going down to ~1.7 nm at 4 ps.
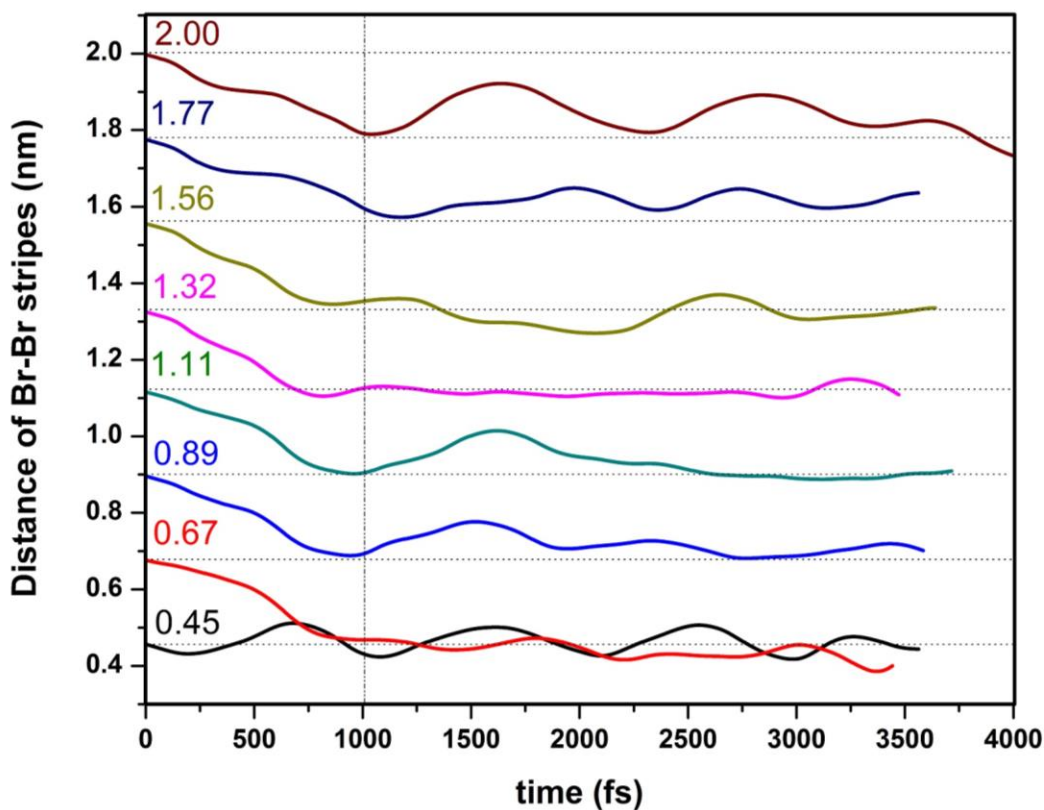
Figure 4. Time evolution of Br-Br stripe distances on Cu(111) by MD simulations starting from the eight equilibrated geometries from 0.45 to 2.0 nm shown in Figure 3a.

We ascribe the Br stripe aggregation partially to the substrate mediation in a thermal bath. Our MD simulation indicates that the total energy almost remained constant (cf.

Figure S2), due to complementary fluctuations between potential and kinetic energies (cf. Figure 5). This may result from the fact that the internal residual force by the thermostat is so small that only the atomic vibrations induce the exchange between potential and kinetic energies. Figure 6 illustrates the strain energy E_{strain} as calculated by the difference between each frozen surface energy from the above complexes (i.e. E_{sub} from Figure 3c) and the Br-free surface energy with full relaxation. The strain energy reflects the surface energy deviation from its equilibrium state and the increase of surface internal energy. The E_{strain} grows from 40 to 90 meV as the longer Br-Br distance increases, due to the formation of three Cu-Br bonds at each different fcc site. The vibrating surface Cu atoms may release thermal energy and weaken the Cu-Br bonds, thus favoring aggregation in fcc sites forming the compact ($\sqrt{3}\times\sqrt{3}$)R30° structure. The surface strain may also play a role in facilitating Br stripe aggregation on Cu(111). Our MD results indicate that the thermal energy of merely 50 K could already significantly widen the Br stripes.
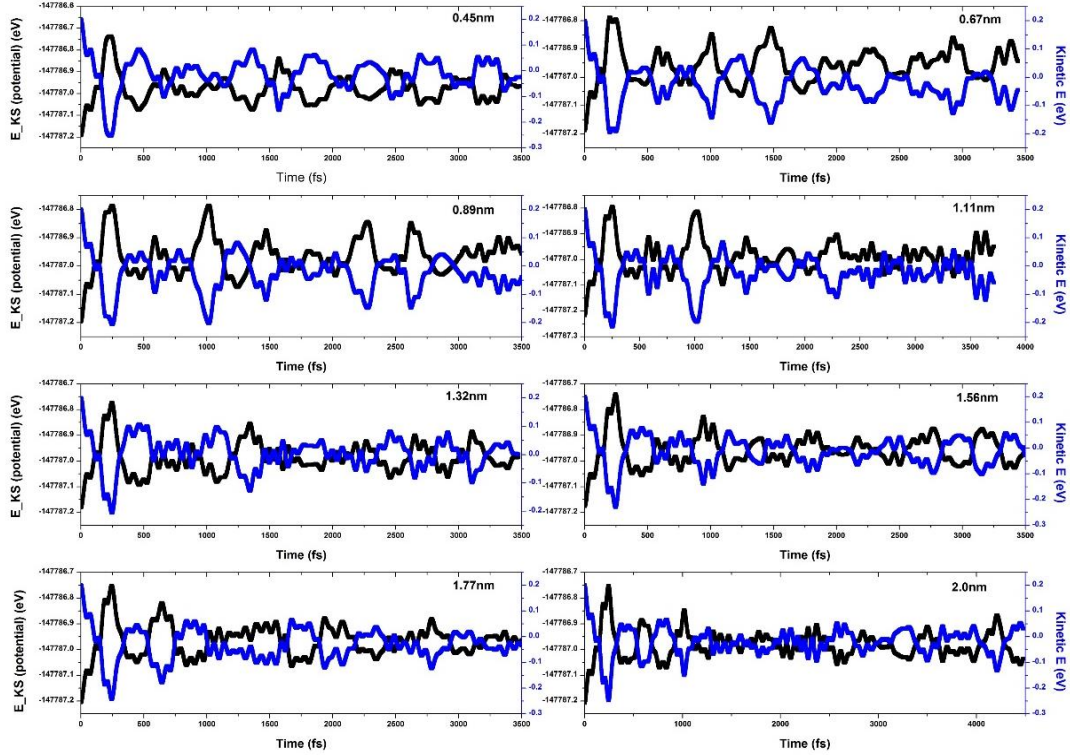

Figure 5. *Time evolutions of complementary fluctuations between potential and kinetic energies of eight complexes for two Br stripes on Cu(111) at distances of 0.25-2 nm by first-principles MD simulations.*
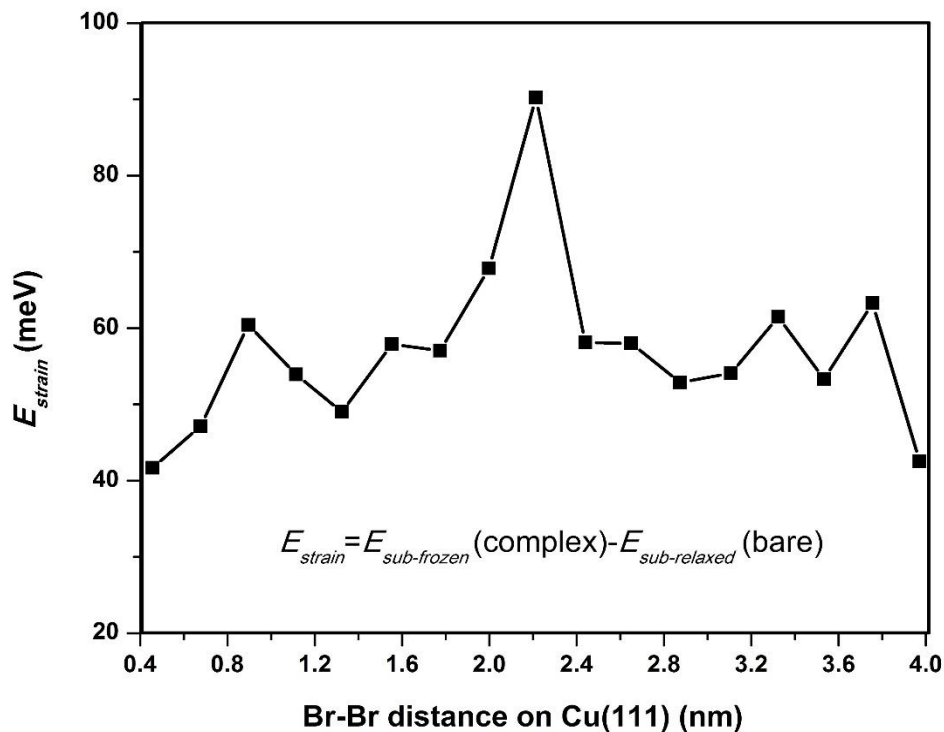
Figure 6. Relative total energies of the frozen substrate from the equilibrated complex with two Br stripe attachments with that of a bare Cu(111) fully relaxed by DFT calculations. The strain energy shows the surface energy deviation from its equilibrium state and its internal energy increase as induced by the formation of Cu-Br covalent bonds.

In addition, the trajectories based on 1000 - ~3500 fs can be used to theoretically predict the pair correlation function, $G(r)$, cf. Figure 7, in order to statistically analyze the favorable Br stripe distance from our MD samples. The reference point is the Br stripe at the left in Figure 3a. We predict the appearance probability of the other Br stripe near fcc sites (i.e. the pair correlation function $G(r)$) in intervals of 0.01 nm. The $G(r)$ peaks are much larger for the 0.45 and 0.67 nm cases than the others. This shows that the Br stripes are favorably aggregated in a distance of 0.45 nm, corresponding to the ($\sqrt{3}\times\sqrt{3}$)R30° structure as dominated by VdW dispersion. Although we do not see Br stripes on surface stabilizing at 1.11 nm during the MD simulations, the $G(r)$ peak appearing at 1.11 nm is relatively higher than the adjacent ones, implying it is likely to be a favorable interval distance between Br stripes.
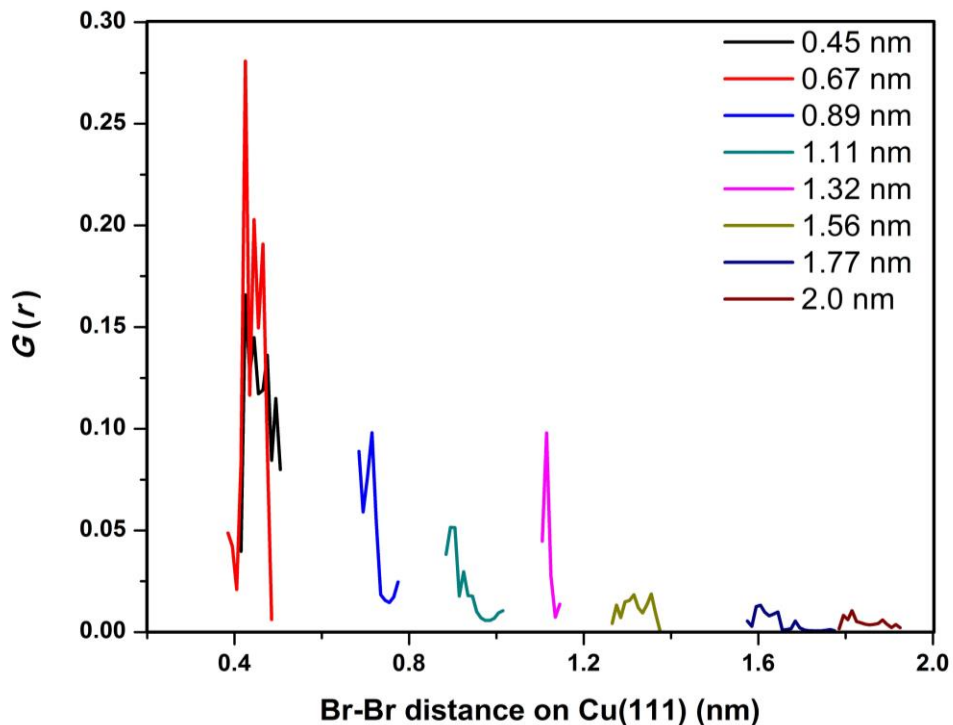
Figure 7. *Pair correlation function, G(r), as a function of Br-Br distance, obtained by analyzing eight MD distance trajectories of Br-Br stripes on Cu(111).*

Combining the influence due to substrate and temperature, we track the evolution of stripe-like electron distributions on the surface with the Br-Br distance, based on the geometries taken from MD simulation frames at 1 ps (cf. the vertical dotted line in Figure 4). As shown in Figure 8, the electron stripes could be generated, merged, separated or removed on Cu(111) with the spacing change of Br stripes. This reflects diverse and changeable formation features for dynamic patterns of Br on Cu(111), which can help to explain why the Br island, stripe and bubble patterns can be found on surfaces.

(a) 0.47 nm   (b) 0.69 nm

(c) 0.90 nm

(d) 1.13 nm

(e) 1.35 nm

(f) 1.60 nm
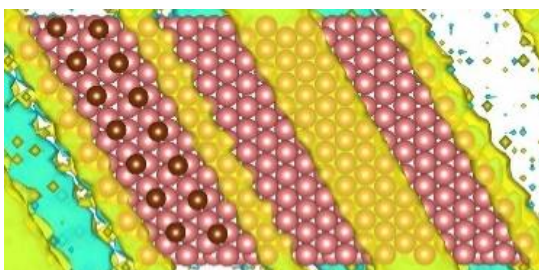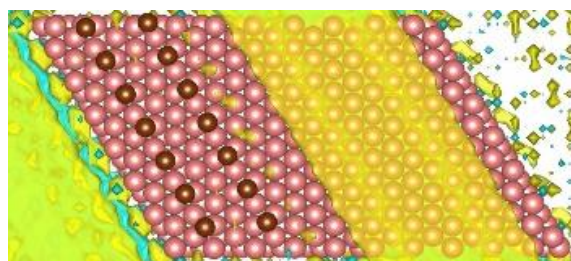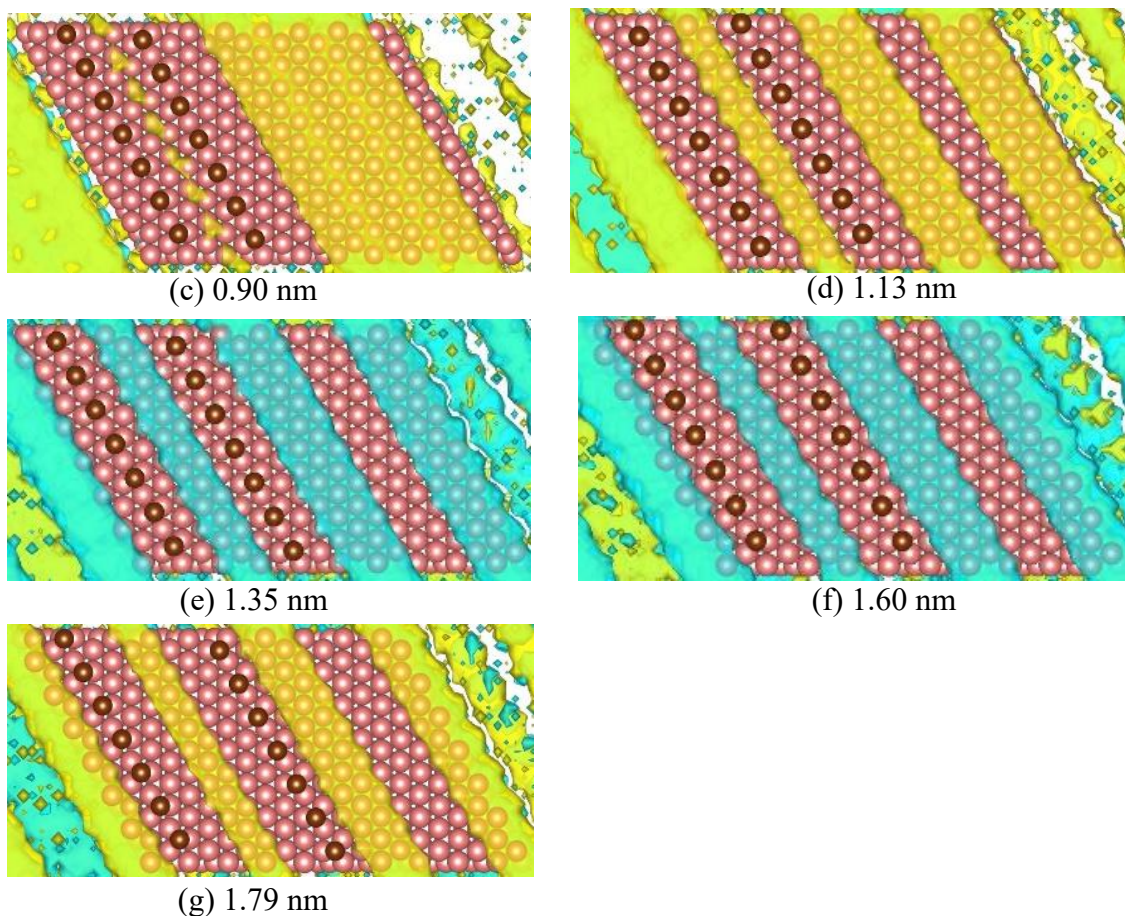
(g) 1.79 nm

Figure 8. *A distinctly stripe-shaped frontier OMO variation with the Br-Br distance from 0.47 (a) to 1.79 nm (g) based on the geometries taken from MD simulation frames at 1 ps at T=50K (cf. Figure S3 (b)-(h)). Noted that each orbital is shown in seven supercells along b direction on a (10√3× √3)R30° unit cell of four-layer Cu(111). Cu and Br atoms are colored in red and brown, respectively. Yellow and blue striped regions represent the MO wave-function with opposite phases. The isovalue is set as 0.01 a.u. to give a clearer illustration.*

4. Conclusion

In conclusion, we have shown that the surface structures of Br stripes on Cu(111) are diverse and changeable, mainly substrate-mediated and temperature-modulated with an integrated impact from molecular orbital interactions and dynamical aggregations, as evidenced by performing first-principles DFT calculations and MD simulations. Specifically, our calculated surface wave-functions in frontier occupied states show stripe-like electron distributions and thus the favorable sites of Br adsorptions on Cu(111) are

stripe-like. A minimum favorable spacing of ~1 nm between stripes was obtained in further total energy calculations in our small-scale model. The temperature effect is also notable in that the thermal energy of 50 K easily dominates Br stripe gathering in $(\sqrt{3}\times\sqrt{3})R30°$ structures, as evidenced by MD simulations of models of Br stripes on Cu(111) surfaces with different neighboring stripe separations varying in the range of 0.45–2 nm. In general, the electron stripes on the surface can be generated, widened, shrunk or removed, also causing spacing changes of Br stripes in a thermal bath, and reflecting diverse and changeable formation features for dynamic patterns of Br on Cu(111).

Acknowledgements

References

[1] M. Seul, D. Andelman, Domain shapes and patterns: the phenomenology of modulated phases, Science 267 (1995) 476–483.

[2] D. Lacoste, T.C. Lubensky, Phase transitions in a ferrofluid at magnetic-field-induced microphase separation, Phys. Rev. E 64 (2001) 041506.

[3] M.F. Islam, K.H. Lin, D. Lacoste, T.C. Lubensky, A.G. Yodh, Field-induced structures in miscible ferrofluid suspensions with and without latex spheres, Phys. Rev. E 67 (2003) 021402.

[4] C.J. Horowitz, M.A. Pérez-García, Neutrino-'pasta' scattering: the opacity of nonuniform neutron-rich matter, Phys. Rev. C 69 (2004) 045804.

[5] F.E. Gabaly, J.M. Puerta, C. Klein, A. Saa, A.K. Schmid, K.F. McCarty, J.I. Cerda, J. de la Figuera, Structure and morphology of ultrathin Co/Ru(0001) films, New J. Phys. 9 (2007) 80.

[6] H.J. Zhao, V.R. Misko, F.M. Peeters, Analysis of pattern formation in systems with competing range interactions, New J. Phys. 14 (2012) 063032.

[7] M.F. Kadodwala, A.A. Davis, G. Scragg, B.C.C. Cowie, M. Kerkar, D.P. Woodruff, R.G. Jones, Structural determination of the Cu(111)-($\sqrt{3}\times\sqrt{3}$)R30°-Cl/Br surface using the normal incidence X-ray standing wave method, Surface Science 324 (1995) 122–132.

[8] R.G. Jones, M. Kadodwala, Bromine adsorption on Cu(111), Surface Science 370 (1997) L219–L225.

[9] J. Inukai, Y. Osawa, K. Itaya, Adlayer structures of chlorine, bromine, and iodine on Cu(111) electrode in solution: in-situ STM and ex-situ LEED studies, J. Phys. Chem. B 102 (1998) 10034–10040.

[10] S.U. Nanayakkara, E.C.H. Sykes, L.C. Fernández-Torres, M.M. Blake, P.S. Weiss, Long-range electronic interactions at a high temperature: bromine adatom islands on Cu(111), Phys. Rev. Lett. 98 (2007) 206108.

[11] W.W. Gao, T.A. Baker, L. Zhou, D.S. Pinnaduwage, E. Kaxiras, C.M. Friend, Chlorine adsorption on Au(111): chlorine overlayer or surface chloride? J. Am. Chem. Soc. 130 (2008) 3560–3565.

[12] C.Y. Nakakura, E.I. Altman, Bromine adsorption, reaction, and etching of Cu(100), Surface Science 370 (1996) 32–46.

[13] Z.V. Zheleva, V.R. Dhanak, G. Held, Experimental structure determination of the chemisorbed overlayers of chlorine and iodine on Au{111}, Phys. Chem. Chem. Phys. 12 (2010) 10754–10758.

[14] K.H. Lau, W. Kohn, Indirect long-range oscillatory interaction between adsorbed atoms, Surface Science 75 (1978) 69.

[15] N. Knorr, H. Brune, M. Epple, A. Hirstein, M.A. Schneider, K. Kern, Long-range adsorbate interactions mediated by a two-dimensional electron gas, Phys. Rev. B 65 (2002) 115420.

[16] M.F. Crommie, C.P. Lutz, D.M. Eigler, Imaging standing waves in a two-dimensional electron gas, Nature 363 (1993) 524–527.

[17] R. Temirov, S. Soubatch, A. Luican, F.S. Tautz, Free-electron-like dispersion in an organic monolayer film on a metal substrate, Nature 444 (2006) 350–353.

[18] I.A. Pašti, S.V. Mentus, Halogen adsorption on crystallographic (111) planes of Pt, Pd, Cu and Au, and on Pd-monolayer catalyst surfaces: first-principles study, Electrochimica Acta 55 (2010) 1995–2003.

[19] Y.H. Duan, S.G. Zhou, Y. Sun, M.J. Peng, The electronic structure and phase diagram of chlorine adsorption on Mg(0001) surface, Comput. Mater. Sci. 84 (2014) 108–114.

[20] L.G.M. Pettersson, P.S. Bagus, Adsorbate ionicity and surface-dipole-moment changes: cluster-model studies of Cl/Cu(100) and F/Cu(100), Phys. Rev. Lett. 56 (1986) 500.

[21] A. Bogicevic, S. Ovesson, P. Hyldgaard, B.I. Lundqvist, H. Brune, D.R. Jennison, Nature, strength, and consequences of indirect adsorbate interactions on metals, Phys. Rev. Lett. 85 (2000) 1910–1913.

[22] T. Roman, A. Groß, Periodic density-functional calculations on work-function change induced by adsorption of halogens on Cu(111), Phys. Rev. Lett. 110 (2013) 156804.

[23] K. Doll, N.M. Harrison, Chlorine adsorption on the Cu(111) surface, Chem. Phys. Lett. 317 (2000) 282–289.

[24] K. Doll, N.M. Harrison, Theoretical study of the chlorine adsorption on the Ag(111) surface, Phys. Rev. B 63 (2001) 165410.

[25] W.L. Zhou, T. Liu, M.C. Li, T. Zhao, Y.H. Duan, Adsorption of bromine on Mg(0001) surface from first-principles calculations, Comput. Mater. Sci. 111 (2016) 47–53.

[26] V.V. Zheltov, V.V. Cherkez, B.V. Andryushechkin, G.M. Zhidomirov, B. Kierren, Y. Fagot-Revurat, D. Malterre, K.N. Eltsov, Structural paradox in submonolayer chlorine coverage on Au(111), Phys. Rev. B 89 (2014) 195425.

[27] J.M. Soler, E. Artacho, J.D. Gale, A. García, J. Junquera, P. Ordejón, D. Sánchez-Portal, The siesta method for ab initio order-N materials simulation, J. Phys.: Condens. Matter 14 (2002) 2745–2779.

[28] M. Dion, H. Rydberg, E. Schröder, D.C. Langreth, B.I. Lundqvist, Van der waals density functional for general geometries, Phys. Rev. Lett. 92 (2004) 246401.

[29] G. Román-Pérez J.M. Soler, Efficient implementation of a van der waals density functional: application to double-wall carbon nanotubes, Phys. Rev. Lett. 103 (2009) 096102.

[30] A. Hauschild, K. Karki, B.C.C. Cowie, M. Rohlfing, F.S. Tautz, M. Sokolowski, Molecular distortions and chemical bonding of a large π-conjugated molecule on a metal surface, Phys. Rev. Lett. 94 (2005) 036106.

[31] R. Coquet, G.J. Hutchings, S.H. Taylor, D.J. Willock, Calculations on the adsorption of Au to MgO surfaces using SIESTA, J. Mater. Chem. 16 (2006) 1978–1988.

[32] A.S. Foster, M.A. Gosálvez, T. Hynninen, R.M. Nieminen, K. Sato, First-principles calculations of Cu adsorption on an H-terminated Si surface, Phys. Rev. B 76 (2007) 075315.

[33] R. Hoffmann, A chemical and theoretical way to look at bonding on surfaces, Rev. Mod. Phys. 60 (1988) 601–628.

[34] R. Car M. Parrinello, Unified approach for molecular dynamics and density-functional theory, Phys. Rev. Lett. 55 (1985) 2471–2474.

[35] P. Ballone, W. Andreoni, R. Car, M. Parrinello, Equilibrium structures and finite temperature properties of silicon microclusters from ab initio molecular-dynamics calculations, Phys. Rev. Lett. 60 (1988) 271–274.

[36] M.D. Segall, P.J.D. Lindan, M.J. Probert, C.J. Pickard, P.J. Hasnip, S.J. Clark, M.C. Payne, First-principles simulation: ideas, illustrations and the CASTEP code, J. Phys.: Condens. Matter 14 (2002) 2717–2744.

[37] G. Csányi, T. Albaret, M.C. Payne, A. de Vita, 'Learn on the fly': a hybrid classical and quantum-mechanical molecular dynamics simulation, Phys. Rev. Lett. 93 (2004) 175503.

[38] O.V. Yazyev, I. Tavernelli, U. Rothlisberger, L. Helm, Early stages of radiation damage in graphite and carbon nanostructures: a first-principles molecular dynamics study, Phys. Rev. B 75 (2007) 115418.

[39] D.B. Ghosh, B.B. Karki, L. Stixrude, First-principles molecular dynamics simulations of $MgSiO_3$ glass: structure, density, and elasticity at high pressure, American Mineralogist 99 (2014) 1304–1314.

[40] S. Nosé, A unified formulation of the constant temperature molecular dynamics methods, J. Chem. Phys. 81 (1984) 511.

[41] S. Nosé, A molecular dynamics method for simulations in the canonical ensemble, Molecular Phys. 100 (2002) 191–198.